PHYSICAL REVIEW D **91,** 065031 (2015)

Gravitational Kaluza-Klein modes in the string-cigar braneworld

D. F. S. Veras,[1,*] J. E. G. Silva,[1,†] W. T. Cruz,[2,‡] and C. A. S. Almeida[1,§]

[1]*Departamento de Física, Universidade Federal do Ceará (UFC), C.P. 6030, Fortaleza 60455-760 Ceará, Brazil*

[2]*Instituto Federal de Educação, Ciência e Tecnologia do Ceará (IFCE) Campus Juazeiro do Norte, CEP 63040-540, Juazeiro do Norte, Ceará, Brazil*

(Received 10 September 2014; published 26 March 2015)

In this work we analyze the properties of the gravitational Kaluza-Klein (KK) modes in two stringlike braneworlds, the thin Gherghetta-Shaposhnikov (GS) model and the thick string-cigar model. The string-cigar model is a smooth generalization of the GS model that undergoes a Ricci geometrical flow. We find a new massless mode in both models satisfying the respective Schrödinger equations. By means of a numerical analysis, we obtain the complete graviton spectrum and its respective eigenfunctions. The KK spectrum exhibits the usual linear regime for large discrete index n and we find a new decreasing regime for small n. Moreover, there is an asymmetric mass gap between the massless mode and the massive KK tower. The mass gap in the GS model is bigger than in the string-cigar model. In addition, the mass gap remains invariant upon the geometrical flow. It turns out that in the string-cigar model the brane structure smoothes and amplifies the KK modes near the brane core. The presence of a potential well in the string-cigar scenario allows the existence of resonant massive gravitons for small masses.

DOI: 10.1103/PhysRevD.91.065031 PACS numbers: 11.10.Kk, 04.50.-h, 11.27.+d, 12.60.-i

I. INTRODUCTION

Among the high energy theories proposed in the last years, the braneworld models gained prominence due to their fundamental basis in string theory and because they provide a solution for the gauge hierarchy and the cosmological constant problems [1–4]. The assumption of extra dimensions proposed by the Kaluza-Klein (KK) models [5] has allowed the development of several models where the four-dimensional observable space-time is regarded as a membrane embedded in a higher-dimensional space-time [6–8]. The Randall-Sundrum (RS) model enhanced this hypothesis by assuming an infinite extra dimension whose warped geometry yields to a compact transverse space [2]. Soon after, some models appeared proposing branes generated by topological defects. In five dimensions, domain walls have been used to represent the brane [7,9,10], whereas in six dimensions, with axial symmetry, the scenario is the so-called stringlike braneworld [11,12].

Stringlike objects, such as the vortices and the cosmic strings, are often described as systems composed by a complex scalar field (global) and gauge field (local) [13]. However, unlike the domain walls, there is not a complete (interior and exterior) stringlike solution analytically known, even in flat space-time. In warped braneworlds, Cohen-Kaplan [14], Gregory [15], and Olaganesi-Vilenkin [16] studied the exterior solution of a global stringlike brane with and without the bulk cosmological constant. The local case was addressed numerically by Giovaninni *et al.* who obtained a smooth geometry satisfying the dominant energy condition [17].

Regardless of the particular model used to compose the brane core, the exterior warped stringlike solution with cosmological constant has a conformally flat behavior that extends the five-dimensional Randall-Sundrum model [18]. In the infinitely thin core brane limit, the resulting scenario is called the Gherghetta-Shaposhnikov (GS) model [19]. This model provides a correction to the Newtonian potential smaller than in the RS model [19]. Moreover, the KK massless mode of the vector gauge field is naturally localized in the GS braneworld [20,21]. The fermionic field, in its turn, requires a minimal coupling with the vector gauge field to localize the massless mode [20–22].

Besides the interesting features of the fields, the stringlike braneworlds also exhibit a rich geometric structure. In fact, the two extra dimensions form a transverse manifold with internal symmetries and properties that reflect on the brane tension and geometry [12]. The transverse manifold used in the GS model is a disc [19]. On the other hand, Kehagias proposed a conical space to provide an explanation for the cosmological constant problem [23]. Garriga-Porrati studied the effects generated by a football-shaped manifold [24] and Gogberashvili *et al.* addressed the fermion generations problem by means of an apple-shaped space [25]. In a supersymmetric model, de Carlos and Moreno found a localized gravity solution without cosmological constant. Since this model considers a geometry that asymptotically has a constant transverse radius, the model is named as a cigarlike universe [26].

*franklin@fisica.ufc.br
†euclides@fisica.ufc.br
‡wilami@pq.cnpq.br
§carlos@fisica.ufc.br

In Ref. [27], the so-called cigar soliton is used to construct an attractive smooth interior and exterior stringlike geometry referred to as the string-cigar model. The cigar soliton is a two-dimensional self-similar solution of the Ricci flow, a geometric flux driven by the Ricci tensor [28,29]. There are important applications of the Ricci flow in different branches of physics as in the sigma models [30], Euclidean black holes [31], topological massive gravity [32], add–drop multiplexer mass [33], and the Heisenberg model in statistical mechanics [34]. The Ricci flow defines a family of geometries developing under an evolution parameter. Therefore, the string-cigar scenario changes its brane properties due to the geometric flow [35]. Since the Ricci soliton extends the Einstein manifolds, the string-cigar geometry can also be realized as an augmented Randjbar-Daemi and Shaposhnikov model [36].

Another smooth stringlike model that leads to a geometrical flow in the transverse space was built with a section of the resolved conifold, an important orbifold in string theory [35]. The string-cigar and the resolved conifold models yield to regular geometries that asymptotically recover the GS model [27]. The string-cigar model satisfies all the regularity conditions required to ensure a well-behaved 3-brane at the origin. In the resolved conifold model, the resolution parameter plays the role of the radius of the fifth dimension that violates the conical behavior near the origin [35].

The string-cigar scenario enables the existence of a localized gravitational massless (or zero) mode that effectively describes the gravity on the brane [27]. The massless mode in this scenario has the same asymptotically exponential behavior of the massless mode in the GS model. Furthermore, near the brane core it has a smooth bell shape [27]. Hence, the string-cigar scenario smoothes the geometry and zero mode near the origin. As the geometry undergoes the Ricci flow in the transverse space, the massless mode changes its width and amplitude [27]. In this work, we find a new massless mode for the GS and the string-cigar models by means of the Schrödinger approach. This new massless mode exhibits a more localized behavior.

Another noteworthy feature of the string-cigar model is its inhomogeneous source [27]. Indeed, the maximum of the stress-energy tensor components is displaced from the origin, which suggests that the brane core is shifted [27]. Giovaninni *et al.* found a similar behavior for an Abelian vortex with a higher winding number [17]. In the string-cigar model, the gravitational massless mode and the energy density share similar profiles. Such behavior shows the influence of the geometric changes on the physics of the brane [27].

As pointed out by Tinyakov and Zuleta, the source for the GS model does not satisfy the dominant energy condition [37]. On the other hand, the string-cigar source undergoes a phase transition whereupon some configurations fulfil all the energy conditions [27]. Furthermore, the string-cigar model recovers the GS one for high values of the bulk cosmological constant.

Nonetheless, the complexity of the differential equation for the KK modes turns the numerical analysis into the most subtle approach to obtain the whole spectrum of masses and eigenfunctions [38]. Thus, the main purpose of this work is to attain the massive KK spectrum and analyze how it behaves on the Ricci flow that the cigar undergoes.

Although Gherghetta and Shaposhnikov have found a complete set of eigenfunctions for a stringlike braneworld, the corresponding KK masses expression for the discrete states is valid only for large values of a discretization index n [19]. In this limit, the masses increase linearly, but for small n the behavior is yet unknown. Using numerical analysis we obtain the complete KK mass spectrum of the GS and string-cigar scenarios. Both models show a decreasing behavior for small n with a mass gap between the linear and decreasing regimes. Moreover, the GS model presents a massive mode with a small mass and amplitude that is absent in the string-cigar model.

The numerical analysis of these two models provides more information on how the fields behave on singular and smooth scenarios in six dimensions. Giovaninni *et al.* have numerically studied the interior and exterior geometry of a stringlike braneworld, but they have not been concerned with the KK spectrum [17]. In this article, we also use numerical methods to find and study gravitational resonant massive modes on both GS and string-cigar models. The analogous Schrödinger potential for the string-cigar model exhibits the usual volcano shape with an infinite potential well around the origin. It turns out that resonant modes are allowed for small masses, in contrast with the GS model where they are absent.

This paper is organized as follows: in Sec. II the main characteristics and results of the GS and string-cigar models are presented. Next, in Sec. III, we present the numerical results which concern to the spectrum and eigenfunction. In Sec. IV, we develop the study of KK massive modes as resonant states. Finally, in Sec. V, some final remarks and perspectives are outlined.

II. STRINGLIKE BRANEWORLDS

Consider a six-dimensional space-time $\mathcal{M}_6$ built from the warped product between a four-dimensional Lorentzian manifold $\mathcal{M}_4$ and a two-dimensional Riemannian manifold $\mathcal{M}_2$. Hereinafter, we refer to $\mathcal{M}_4$ as a 3-brane and $\mathcal{M}_2$ as the transverse space. A stringlike braneworld is a static six-dimensional $\mathcal{M}_6$ with an axial symmetry in the transverse space. A subtle metric for this model is given by [12,14–17,19,20]

$$\begin{aligned} ds_6^2 &= g_{AB}(x,\rho,\theta)dx^A dx^B \\ &= \sigma(\rho)g_{\mu\nu}(x)dx^\mu dx^\nu - d\rho^2 - \gamma(\rho)d\theta^2, \end{aligned} \tag{1}$$

where x are brane coordinates, $\rho \in [0, \infty)$ and $\theta \in [0, 2\pi]$ are the extra dimensions, and σ and γ are the so-called warp factors.

The additional regularity conditions,

$$\sigma(0) = 1, \qquad \sigma'(0) = 0,$$
$$\gamma(0) = 0, \qquad (\sqrt{\gamma(0)})' = 1, \tag{2}$$

are imposed in order to avoid singularities [12], where the $(')$ stands for the derivative ∂_ρ. The conditions for σ in Eq. (2) are already present in the RS models [1,2], whereas the further assumption for γ reflects the smooth correction behavior near the origin [12,17,19,37].

Regardless of the particular model for the source, an axisymmetric stress-energy tensor is adopted as follows [12,17,19]:

$$T^A_B = \mathrm{diag}(t_0, t_0, t_0, t_0, t_\rho, t_\theta). \tag{3}$$

For a global string, for instance, $t_\rho = -t_\theta$ [14–16]. In the presence of a bulk cosmological constant Λ and for a flat brane $\mathcal{M}_4$, the Einstein equation reads

$$R_{ab} - \frac{R}{2} g_{ab} = -\kappa_6(\Lambda g_{ab} + T_{ab}), \tag{4}$$

which for the metric ansatz (1) yields to

$$\frac{3}{2}\left(\frac{\sigma'}{\sigma}\right)' + \frac{3}{2}\left(\frac{\sigma'}{\sigma}\right)^2 + \frac{3}{4}\frac{\sigma'}{\sigma}\frac{\gamma'}{\gamma} + \frac{1}{4}\left(\frac{\gamma'}{\gamma}\right)^2 + \frac{1}{2}\left(\frac{\gamma'}{\gamma}\right)' = -\kappa_6(\Lambda + t_0(\rho)), \tag{5}$$

$$\frac{3}{2}\left(\frac{\sigma'}{\sigma}\right)^2 + \frac{\sigma'}{\sigma}\frac{\gamma'}{\gamma} = -\kappa_6(\Lambda + t_\rho(\rho)), \tag{6}$$

$$2\left(\frac{\sigma'}{\sigma}\right)' + \frac{5}{2}\left(\frac{\sigma'}{\sigma}\right)^2 = -\kappa_6(\Lambda + t_\theta(\rho)), \tag{7}$$

where κ_6 is the six-dimensional gravitational constant related to the six-dimensional energy scale by $\kappa_6 = \frac{8\pi}{M_6^4}$ [27].

Let us analyze the vacuum configuration. The third Einstein equation (7) provides

$$2\left(\frac{\sigma'}{\sigma}\right)' + \frac{5}{2}\left(\frac{\sigma'}{\sigma}\right)^2 = -\kappa_6\Lambda. \tag{8}$$

Defining

$$y(\rho) = \frac{\sigma'}{\sigma}, \tag{9}$$

Eq. (8) turns out to be

$$y' + \frac{5}{4}y^2 - \frac{\kappa_6|\Lambda|}{2} = 0, \tag{10}$$

the solution of which is

$$y(\rho) = c\tanh\frac{5c}{4}(\rho + \rho_0), \tag{11}$$

where

$$c^2 = -\frac{2\kappa_6}{5}\Lambda, \tag{12}$$

and ρ_0 is an integration constant. Integrating Eq. (11) yields to the warp factor

$$\sigma(\rho) = \sigma_0 \cosh^{\frac{4}{5}}\left(\frac{5}{4}c\rho\right), \tag{13}$$

with an integration constant σ_0. Substituting the warp factor (13) into the Einstein equations and imposing the regularity conditions (2), we obtain the angular metric component γ:

$$\gamma(\rho) = \left(\frac{4}{5c}\right)^2 \sinh^2\left(\frac{5c\rho}{4}\right)\sigma^{-\frac{3}{2}}. \tag{14}$$

The warp factor in (13) and the angular metric component in (14) provide an infinite volume to the transverse space that leads to a non–four-dimensional effective gravitational theory.

The relation between the bulk Planck mass M_6 and the brane Planck masses M_4 is given by

$$M_4^2 = 2\pi M_6^4 \int_0^\infty \sigma(\rho)\sqrt{\gamma(\rho)}d\rho. \tag{15}$$

Then, for a stringlike model described by the warp function (13) and the angular metric component (14), the brane Planck scale diverges.

Another important characteristic of the stringlike models is the string tensions μ_i defined by [17,19]

$$\mu_i(c) = \int_0^\epsilon t_i(\rho, c)\sigma^2(\rho, c)\sqrt{\gamma(\rho, c)}d\rho, \tag{16}$$

which determines the matching between an internal and external geometric solution, where ϵ is the width of the core [12,17,19].

Once we have presented the general aspects of the stringlike scenario, we study the behavior of the small metric fluctuations around this configuration.

Performing the following conformal invariant perturbation [17,19,27,39],

$$ds_6^2 = \sigma(\rho)(\eta_{\mu\nu} + h_{\mu\nu}(x,\rho))dx^\mu dx^\nu + d\rho^2 + \gamma(\rho)d\theta^2, \tag{17}$$

the first-order perturbed Einstein equation (4) yields to [17,19,27,39]

$$\Box_6 h_{\mu\nu} = \partial_A(\sqrt{-g_6}\eta^{AB}\partial_B h_{\mu\nu}) = 0. \tag{18}$$

Thus, the tensorial perturbation $h_{\mu\nu}$ can be regarded as a tensorial field (graviton) propagating in the bulk.

Assuming the usual Kaluza-Klein decomposition [2,19,20,27]

$$h_{\mu\nu}(x,\rho,\theta) = \sum_{l,m=0}^{\infty} \phi_{m,l}(\rho)e^{il\theta}\hat{h}_{\mu\nu}(x), \tag{19}$$

and a free-wave dependence on the 3-brane

$$\Box_4 h_{\mu\nu}(x^\xi) = m_0^2 h_{\mu\nu}(x^\xi), \tag{20}$$

the graviton equation of motion (18), for a conformal scenario where $\gamma(\rho) = \sigma(\rho)\beta(\rho)$, reads [19,27]

$$(\sigma^{\frac{5}{2}}\sqrt{\beta}\phi'_{m,l}(\rho))' + \sigma^{\frac{3}{2}}\sqrt{\beta}\left(m_0^2 - \frac{l^2}{\beta^2}\right)\phi_{m,l}(\rho) = 0. \tag{21}$$

The function β is responsible for the conical behavior [27,35]. Equation (21) describes the radial behavior of the graviton on stringlike scenarios. The presence of the angular number l turns the spectrum degenerated [19]. In addition, due to the axial symmetry, the boundary conditions are [17,19,27]

$$\phi'(0) = \phi'(\infty) = 0. \tag{22}$$

The radial equation (21) and the boundary conditions (22) provide a set of solutions whose orthogonality relation is given by

$$\int_0^\infty \sigma^{\frac{3}{4}}\sqrt{\beta}\phi_{m,l}\phi_{n,l'}d\rho = \delta_{mn}\delta_{ll'}. \tag{23}$$

The eigenvalues of Eq. (21) satisfying the boundary conditions (22) are called the KK spectrum (mass) and the respective eigenfunctions are called the KK states. Among the KK states there is one for a vanishing mass, called massless or zero mode. From Eq. (21), the massless mode has the form

$$\phi_0(\rho) = A_1\int_0^\rho \sigma^{-\frac{5}{2}}\beta^{-\frac{1}{2}}d\rho' + A_2, \tag{24}$$

where A_1 and A_2 are constants. A similar massless mode was found by Csaki *et al.* for nonconformally flat space-times [39].

A suitable way to study the KK spectrum consists of turn Eq. (21) into a Schrödingerlike equation [9,10,14,27,38–40]. By taking the change of independent variable [27]

$$z(\rho) = \int^\rho \sigma^{-1/2}d\rho' \tag{25}$$

and of a dependent variable

$$\phi_m(z) = u(z)\Psi_m(z), \tag{26}$$

where

$$\frac{\dot{u}}{u} + \frac{\dot{\sigma}}{\sigma} + \frac{1}{4}\frac{\dot{\beta}}{\beta} = 0, \tag{27}$$

for which the overdot means derivatives with respect to the z coordinate, the radial equation (21) yields to

$$-\ddot{\Psi}_m(z) + U(z)\Psi_m(z) = m^2\Psi_m(z), \tag{28}$$

where

$$U(z) = \frac{\ddot{\sigma}}{\sigma} + \frac{1}{2}\frac{\dot{\sigma}}{\sigma}\frac{\dot{\beta}}{\beta} - \frac{3}{16}\left(\frac{\dot{\beta}}{\beta}\right)^2 + \frac{1}{4}\frac{\ddot{\beta}}{\beta} + \frac{l^2}{\beta}. \tag{29}$$

The boundary conditions (22) imply the following boundary conditions for $\Psi(z)$:

$$\begin{aligned} u'(0)\Psi(0) + u(0)\Psi'(0) = 0, \\ u'(\infty)\Psi(\infty) + u(\infty)\Psi'(\infty) = 0. \end{aligned} \tag{30}$$

Besides the bijective relation between the Sturm-Liouville and Schrödinger approaches, the last method provides information about resonant modes that we consider in Sec. IV. In the following, we study the geometrical features and the properties of Eq. (21) in the GS model and the string-cigar model.

A. The GS model

Gherghetta and Shaposhnikov found a vacuum solution of the Einstein equations that localizes the gravity on the stringlike brane [19]. Assuming that [19]

$$\frac{\sigma'}{\sigma} = -c, \tag{31}$$

which can be obtained from the hyperbolic tangent function in Eq. (11) in one of its asymptotic values, Eq. (8) yields to the following warp function:

$$\sigma(\rho) = \mathrm{e}^{-c\rho}. \tag{32}$$

Moreover, for

$$\beta(\rho) = R_0^2, \tag{33}$$

the GS model describes a AdS_6 space-time [19]. Since the GS model is built from the vacuum solution, it can be regarded as the space-time of a thin stringlike braneworld [17,37]. In addition, the GS solution does not satisfy the regularity conditions at the origin presented in Eq. (2).

In the GS model, the graviton obeys the radial equation [19]

$$\phi_m'' - \frac{5}{2}c\phi_m' + (m_0^2 - l^2/R_0^2)\mathrm{e}^{c\rho}\phi_m = 0. \tag{34}$$

Changing the independent variable to $u = \frac{2m}{c}\mathrm{e}^{\frac{c}{2}\rho}$ and the dependent variable to $\phi_m = \mathrm{e}^{\frac{5}{4}c\rho}\chi_m$, the χ_m function satisfies the Bessel differential equation

$$\frac{d^2\chi_m}{du^2} - \frac{1}{u}\frac{d\chi_m}{du} + \left[1 - \left(\frac{5}{2}\right)^2\frac{1}{u^2}\right]\chi_m = 0. \tag{35}$$

Thus, the general solution of Eq. (34) can be written as [19]

$$\phi_m(\rho) = \mathrm{e}^{\frac{5}{4}c\rho}\left[B_1 J_{5/2}\left(\frac{2m}{c}\mathrm{e}^{\frac{1}{2}c\rho}\right) + B_2 Y_{5/2}\left(\frac{2m}{c}\mathrm{e}^{\frac{1}{2}c\rho}\right)\right], \tag{36}$$

where B_1 and B_2 are arbitrary constants and $m = m_0^2 - l^2/R_0^2$. This solution grows exponentially, revealing that massive modes are not localized on the brane [19].

From Eq. (24), the general GS massless mode has the form

$$\phi_0(\rho) = A_1\mathrm{e}^{\frac{5}{2}c\rho} + A_2. \tag{37}$$

Among the two solutions in Eq. (37), only $\phi_0 = A_2$ satisfies the orthogonality relation (23) [19]. Then Gherghetta and Shaposhnikov defined an orthonormal solution by [19]

$$\psi_m(\rho) = \mathrm{e}^{-\frac{3}{4}c\rho}\phi_m(\rho), \tag{38}$$

so that the zero mode becomes

$$\psi_0(\rho) = \sqrt{\frac{3c}{2R_0}}\mathrm{e}^{-\frac{3}{4}c\rho}. \tag{39}$$

The massless mode in Eq. (39) is localized in the thin-string brane [19]. However, this solution does not satisfy the boundary conditions (22) at $\rho = 0$, because the warp factor (32) does not obey the usual regularity conditions.

On the other hand, by means of the Schrödinger approach, we find another more localized massless mode. Indeed, the Schrödinger equation (28) for the GS model is given by

$$-\ddot{\Psi}_m + \frac{6}{z^2}\Psi_m = m^2\Psi_m, \tag{40}$$

where $z = \frac{2}{c}\mathrm{e}^{\frac{c}{2}\rho}$ and by Eq. (27), the relation between ϕ_m and Ψ_m is

$$\phi_m = C_0\mathrm{e}^{c\rho}\Psi_m. \tag{41}$$

For $m = 0$, Eq. (40) has the solutions

$$\begin{aligned}\Psi_0 &= C_1 z^3 + C_2 z^{-2} \\ &= C_1\mathrm{e}^{\frac{3}{2}c\rho} + C_2\mathrm{e}^{-c\rho},\end{aligned} \tag{42}$$

which, using Eq. (41), yields to the zero mode (37). In order for Ψ_0 to be normalized, we set $C_1 = 0$. Therefore, we find a localized zero mode satisfying the analogous Schrödinger equation in the GS model given by

$$\Psi_0(\rho) = \sqrt{\frac{7c}{2R_0}}\mathrm{e}^{-c\rho}. \tag{43}$$

It is worthwhile to mention that at the origin, the zero mode Ψ_0 in Eq. (43) is higher than the zero mode ψ_0 proposed in Ref. [19]. The rate of decay of the zero mode Ψ_0 is also higher than the zero mode ψ_0. Furthermore, the massless mode (43) satisfies the boundary conditions (30).

The solution of the GS model Schrödinger-like equation for $m \neq 0$ is

$$\begin{aligned}\Psi_m(z) = &\sqrt{\frac{2}{m\pi}}\left(\frac{1}{mz}\right)^2 \\ &\times [(m^2z^2 - 3mz - 3)(\cos(mz) - \sin(mz))].\end{aligned} \tag{44}$$

Since $\Psi_m(z)$ is not defined for $m = 0$, we cannot obtain the massless mode (43) from the massive mode in Eq. (44). This shows a mass gap in the GS model that we explore numerically in Sec. III. Moreover, in the asymptotic limit, the massive modes Ψ_m assume the plane wave form given by

$$\Psi_m(z \to \infty) = \sqrt{\frac{2}{m\pi}}(\cos(mx) - \sin(mx)). \tag{45}$$

Since the massive modes are not normalizable, the KK spectrum can be obtained only by inserting a finite radial distance cutoff $\rho_{\max}$ and imposing the boundary conditions (22) [19,20]. As performed in Ref. [20], the spectrum is obtained by the zeros of the Bessel function

$$J_{\frac{3}{2}}\left(\frac{2m_{\tilde{n}}}{2}e^{\frac{c}{2}\rho_{\max}}\right)=0 \tag{46}$$

that for large index $\tilde{n}$ yields to [19]

$$m_{\tilde{n}} \simeq c\left(\tilde{n}-\frac{1}{2}\right)\frac{\pi}{2}e^{-\frac{c}{2}\rho_{\max}}. \tag{47}$$

The linear relation between the mass and the index $\tilde{n}$ is rather important in the Newtonian potential correction [19]. Nevertheless, the formula (47) is valid only for great values of the discrete index $\tilde{n}$ [19]. In Sec. III we obtain the eigenfunctions of the GS model and a complete spectrum $m_{\tilde{n}}$.

It is worthwhile to mention that the massive KK spectrum in Eq. (47) is strongly dependent on the cutoff distance $\rho_{\max}$. For a model with finite radial coordinate $0 \leq \rho \leq R$, the cutoff distance is $\rho_{\max}=R$. Note that when the cutoff distance $\rho_{\max}$ increases, the magnitude of the KK masses, given by expression (47), is reduced. For an infinite radial coordinate ρ, the KK spectrum $m_{\tilde{n}}$ vanishes for all $\tilde{n}$ [20]. Thus, $m_0^2=(\frac{l}{R_0})^2$, i.e., the KK masses depend only on the angular number l, which is similar to the factorizable Kaluza-Klein model expression for the massive spectrum.

B. The string-cigar model

An extension to the GS model, the so-called string-cigar braneworld [27], is built from a warped product between the 3-brane and cigar soliton space [27]. The cigar soliton is a two-dimensional stationary solution for the Ricci flow

$$\frac{\partial}{\partial\lambda}g_{ab}(\lambda)=-2R_{ab}(\lambda), \tag{48}$$

where λ is a metric parameter and R_{ab} is the Ricci tensor [28]. An axisymmetric metric for the cigar soliton can be written as [29]

$$ds_\lambda^2=d\rho^2+\frac{1}{\lambda^2}\tanh^2(\lambda\rho)d\theta^2. \tag{49}$$

It is straightforward to see that the cigar soliton is a smooth manifold.

The main idea of the string-cigar model is to use the cigar soliton as the transverse space in order to smooth the GS model [27]. The Ricci flow defines a family of stringlike branes whose evolution of the transverse space yields to variations on the physical properties of the brane [27]. Since the asymptotic value of the scalar curvature depends on the evolution parameter [27], the geometric flow represents a variation of the bulk cosmological constant. Then λ and c can be regarded as equivalent evolution parameters. The string-cigar scenario is asymptotically flat, as well as the disc of radius $1/\lambda=R_0$ used in the GS model [28]. However, near the origin, the $\tanh^2\rho$ term smoothes the geometry and provides a thickness to the brane [27].

The warp factor and the angular metric component proposed are, respectively, [27]

$$\sigma(\rho,c)=e^{-(c\rho-\tanh(c\rho))} \tag{50}$$

and

$$\gamma(\rho,c)=\frac{1}{c^2}\tanh^2(c\rho)\sigma(\rho,c). \tag{51}$$

The metric (1) with Eqs. (50)–(51) represents a spacetime inside and outside a stringlike defect that satisfies all the regularity conditions [27].

The Einstein equation provides the stress-energy tensor components [27]:

$$t_0(\rho,c)=\frac{c^2}{\kappa_6}\left(7\mathrm{sech}^2c\rho+\frac{13}{2}\mathrm{sech}^2c\rho\tanh k\rho-\frac{5}{2}\mathrm{sech}^4c\rho\right), \tag{52}$$

$$t_\rho(\rho,c)=\frac{c^2}{\kappa_6}\left(5\mathrm{sech}^2c\rho+2\mathrm{sech}^2c\rho\tanh c\rho-\frac{5}{2}\mathrm{sech}^4c\rho\right), \tag{53}$$

$$t_\theta(\rho,c)=\frac{c^2}{\kappa_6}\left(5\mathrm{sech}^2c\rho+4\mathrm{sech}^2c\rho\tanh c\rho-\frac{5}{2}\mathrm{sech}^4c\rho\right). \tag{54}$$

The components are all non-negative and dependent on the evolution parameter c [27]. In Ref. [27], a detailed analysis showed that, as long as the geometry undergoes the Ricci flow, the source passes through different phases, all of them satisfying the weak, strong and dominant energy conditions [27]. Since c is related to the cosmological constant, the Ricci flow governs how a flow of the bulk cosmological constant changes the source of this smoothed stringlike braneworld [27].

Figure 1 shows the energy density $t_0(\rho,c)$ for some values of the evolution parameter. It is important to mention that the core is shifted from the origin. A similar behavior was found by Giovannini *et al.* for an Abelian vortex braneworld [17]. Giovannini *et al.* considered the vortex generated by a $\lambda\phi^4$ potential [17]; we argue that the string-cigar model can be generated by a vortex with a deformed potential. The width of the core of the brane ϵ can be estimated as $\epsilon=\bar{\rho}$, where $\bar{\rho}$ stands for the half-maximum position of t_0. Furthermore, the higher the value of c, the smaller the width of the core ϵ. Then, for $c\to\infty$, the string-cigar solution approaches the GS model.

In the string-cigar geometry, the radial KK equation takes the form

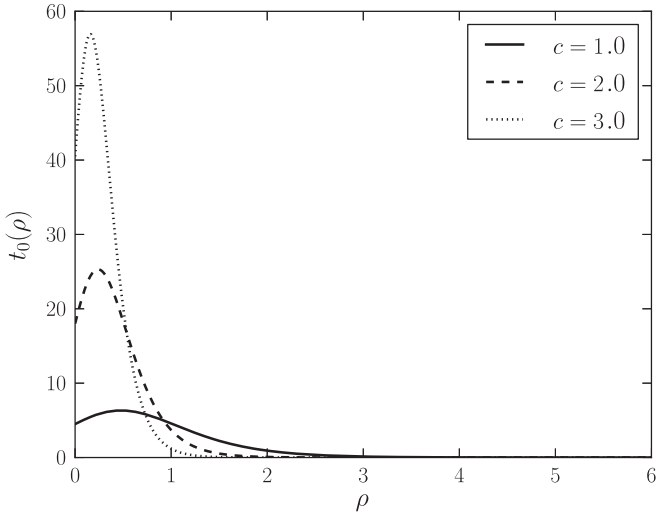

FIG. 1. Energy density of the string-cigar braneworld.

$$\phi_m'' + c\left[-\frac{5}{2}\tanh^2(c\rho) + \frac{\mathrm{sech}^2(c\rho)}{\tanh(c\rho)}\right]\phi_m' + \mathrm{e}^{(c\rho-\tanh(c\rho))}\left(m_0^2 - \frac{l^2c^2}{\tanh^2(c\rho)}\right)\phi_m = 0. \quad (55)$$

Note that the mass term has a radial dependence that diverges at the origin and converges asymptotically to the GS value. For $\rho \to \infty$, Eq. (55) has the same form of Eq. (34), with a rescaled mass $m \to \mathrm{e}^{-1/2}m$. Hence, the asymptotic solutions of (55) have the same behavior of Eq. (36) [27].

Following the Schrödinger approach, we can redefine the KK eigenfunctions by

$$\phi_m = \sigma(\rho, c)\left(\frac{\tanh c\rho}{c}\right)^{1/4}\Psi_m, \quad (56)$$

and the independent variable by

$$z = z(\rho) = \int^{\rho} \mathrm{e}^{\frac{c\rho' - \tanh c\rho'}{2}} d\rho'. \quad (57)$$

The transformation (57) cannot be written explicitly. However, it turns out that, for $m = 0$, the solution of the Schrödinger equation is given by [27]

$$\Psi_0(\rho, c) = N\sigma(\rho, c)\left(\frac{\tanh c\rho}{c}\right)^{1/4}, \quad (58)$$

where N is a normalization factor. The solution (58) can be realized as a smoothed GS massless mode (37). Indeed, in the string cigar the massless mode has the same asymptotic behavior of the GS massless mode. On the other hand, in contrast with the GS model, the string-cigar massless mode vanishes at the origin because of the conical behavior provided by the $\tanh c\rho$ factor. This behavior agrees with the shift of the brane core.

The complexity of the radial equation (55) makes necessary the use of numerical methods to derive solutions for the complete domain. The numerical solutions are presented in Sec. III. Moreover, the Schrödinger-like equation (28) for the string-cigar scenario must be solved on the z coordinate, which may not be written down explicitly. The numerical solutions for the KK modes in the string-cigar model are presented in Sec. IV. Nevertheless, the analogue quantum potential (29) may be expressed as a function of ρ:

$$\bar{U}(\rho) = c^2\left(\frac{3}{2}\tanh^2 c\rho - \frac{9}{4}\mathrm{sech}^2 c\rho \tanh c\rho - \frac{1}{4}\frac{\mathrm{sech}^4 c\rho}{\tanh c\rho} - \mathrm{sech}^2 c\rho\right)\mathrm{e}^{-(c\rho-\tanh c\rho)} + \frac{c^2l^2}{\tanh^2 c\rho}. \quad (59)$$

III. MASS SPECTRUM AND KK EIGENFUNCTIONS

We solved the KK equations (34) and (55) by the matrix method [41] with second-order truncation error in order to attain the complete KK spectra of the GS and string-cigar scenarios. Since the angular number l leads to a degenerate spectrum, we are interested in the $l = 0$ solutions (which are referred to s waves). Henceforward, we label the graviton mass as m instead of m_0. Furthermore, the present Sturm-Liouville problems are extremely sensible on c parameter variations due to the exponential terms. Then, in order to prevent overflow errors, we fixed $c = 1.0$. For the GS model, the domain ρ was discretized in [0.0, 5.7] with $N = 500$ uniform subdivisions. However, since Eq. (55) is singular at the origin, and the first- (zeroth-) order derivative coefficient is strongly active for small (large) ρ values, the optimum domain for the string-cigar model is [0.01, 5.70].

The number of subdivisions of the interval $[a, b = \rho_{\max}]$, n, is intrinsically related with the number of zeros of the Bessel function $\tilde{n}$ in this range. In fact, the higher n is, the more zeros exist in the interval. These zeros split the interval into a partition. Therefore, the eigenvalues m_n are labeled by the number of subdivisions. Henceforward, n and $\tilde{n}$ are equivalent labels.

Figures 2–3 show the complete spectrum m_n for GS and string-cigar models, respectively. The eigenvalues are all real and thus the models do not carry tachyons. For large values of the discretization index n (on the present case, $n > 455$) the mass spectrum for both models grows linearly, which agrees with the GS model [19]. On the

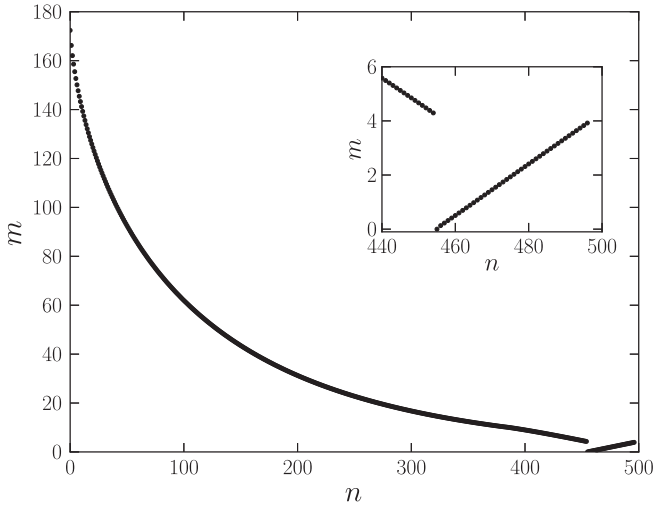

FIG. 2. GS model mass spectrum obtained by the matrix method. The subgraph is the linear regime scale magnification.

other hand, for $n \leq 455$, the mass values decrease as $m_n \approx \frac{1}{n}$, an important new behavior that can lead to corrections on the Newtonian potential [19]. The decreasing behavior for small n agrees with the analytical expression for the zeros of the Bessel functions $J_{\frac{3}{2}}(\frac{2m_n}{c}e^{\frac{1}{2}c\rho}) = 0$, namely [42],

$$m_n = \frac{c}{2}\left[\left(n-\frac{1}{2}\right)\pi + \frac{1}{4[(n-\frac{1}{2})\pi]} + \cdots\right]e^{-\frac{c\rho}{2}}. \quad (60)$$

Hence, for small n, the decreasing behavior prevails over the linear regime.

For $n = 455$, the minimum mass value is $m_{455} = 5.172 \times 10^{-7}$, rather small compared to the whole

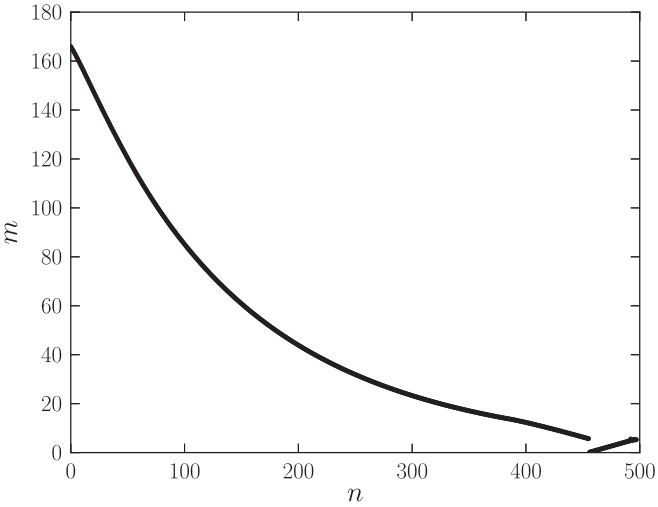

FIG. 3. Mass spectrum of the string-cigar model obtained by the matrix method. It is very similar to the GS model except for the absence of a transient state.

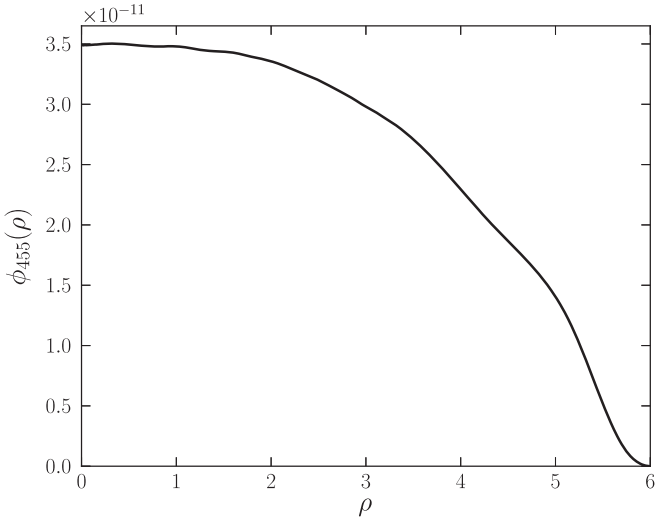

FIG. 4. GS model numerical eigenfunction for $m = 5.172 \times 10^{-7}$.

set. The respective eigenfunction ϕ_{455} is plotted in Fig. 4. This eigenfunction possesses a tiny amplitude and is similar to the GS localized massless mode. Then this massive state can be seen as a transient state between the massless mode and the massive KK tower. However, unlike the GS zero mode, the ϕ_{455} satisfies the boundary conditions (22).

The numerical analysis revealed another feature of the GS model not present in Ref. [19], a mass gap between the decreasing and linear regimes. It turns out that there are two asymmetric mass gaps on the GS model between the transient state m_{455} and its neighbors in the massive KK tower. Table I shows that the difference between m_{455} and m_{456} is higher than the subsequent ones that are approximately $\delta m \approx 0.094$. Therefore, the transition between the decreasing and linear regimes is not continuous and passes through a transient state of tiny mass.

The existence of a mass gap and the transient massive mode agrees with the analytical solutions for the massive modes (36) and for the massless mode (37). Indeed, for small masses it can expand the massive mode as

$$\phi_{m\to 0}(\rho) = D_1\left(\frac{c}{2m}\right)^{\frac{5}{2}} + D_2\left(\frac{c}{2m}\right)^{\frac{1}{2}}e^{c\rho} + D_3\left(\frac{2m}{c}\right)^{\frac{1}{2}}e^{\frac{3}{2}c\rho} + \mathcal{O}\left(e^{\frac{5}{2}c\rho}\right), \quad (61)$$

TABLE I. Some mass eigenvalues for high values of the discretization index where the linear regime (for $n > 455$) is noticeable. The smallest mass value m_{455} corresponds to the transient state.

$m_{454} = 4.295$	$m_{458} = 0.317$
$m_{455} = 5.172 \times 10^{-7}$	$m_{459} = 0.411$
$m_{456} = 0.130$	$m_{460} = 0.504$
$m_{457} = 0.224$	$m_{461} = 0.598$

where D_1, D_2, and D_3 are constants determined by the constants B_1 and B_2 and the expansion of the Bessel functions at the origin. It is worthwhile to say that since $\lim_{m\to 0}\phi_m(\rho) = +\infty$, it is not possible to continuously attain the massless mode (37) from the massive mode expression (36). Thus, there is a mass gap between the massless and the first massive modes. Furthermore, the small amplitude of ϕ_{455} can be explained by the small values of the constants, e.g., $D_3 \approx 10^{-32}$, and by the boundary conditions that relate the constants.

The string-cigar mass spectrum is very similar to the GS one, except for the absence of the transient massive mode. Thus, the near brane correction driven by the conical geometry provides a more regular gravitational massive spectrum. Furthermore, it turns out that the mass gap remained invariant for all the values of c used. This feature suggests that the geometrical flow does not break the discontinuity between the two regimes.

The eigenfunctions of the GS and string-cigar models were plotted for some mass eigenvalues in Figs. 5–6, respectively. As expected, the massive solutions for both models match the same behavior asymptotically. Near the origin, the amplitude of the massive modes in the string-cigar model is bigger than the amplitude of the massive modes in the GS model. Moreover, they are smooth in the core and near the brane, as obtained in Ref. [27] by qualitative analysis. Around the origin the string-cigar eigenfunctions behave as Bessel functions of the first kind $J_0(m\rho)$. Indeed, a first-order expansion of the coefficients of Eq. (55) at the origin yields

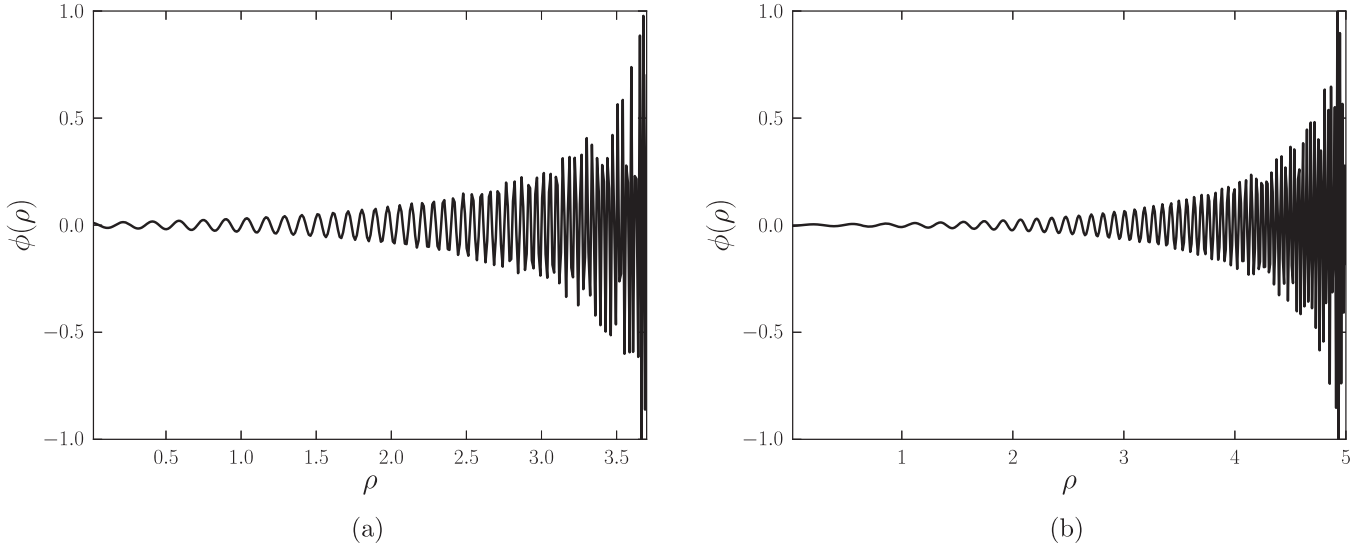

FIG. 5. GS model numerical eigenfunction for (a) $m = 37.156$ and (b) $m = 22.729$.

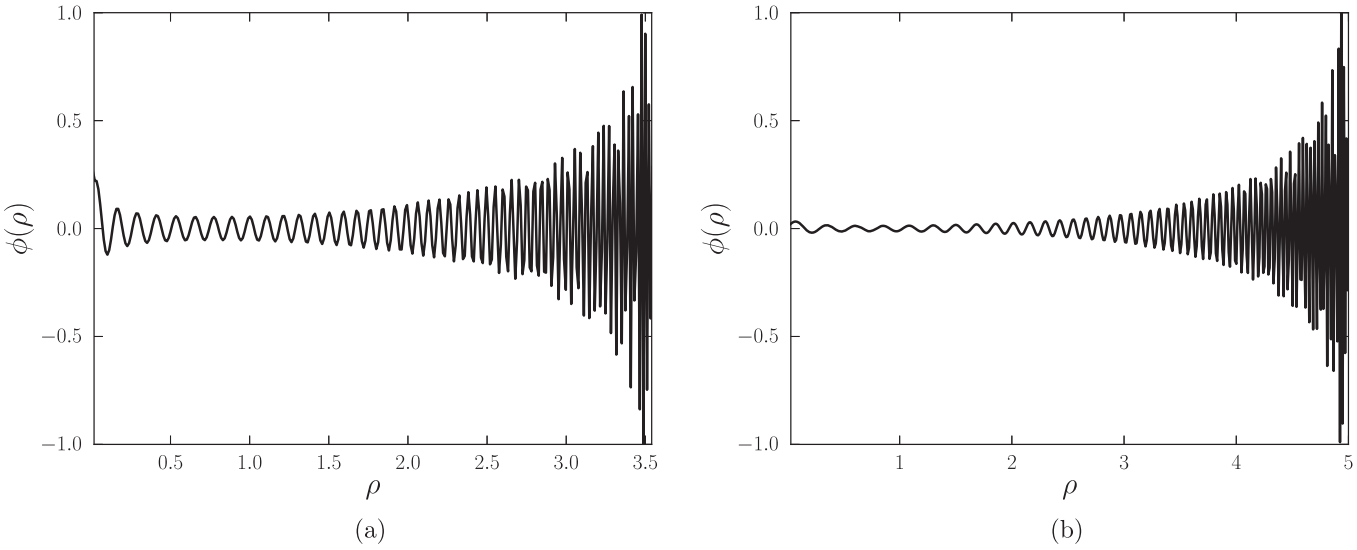

FIG. 6. String-cigar model numerical eigenfunction for (a) $m = 37.022$ and (b) $m = 22.721$.

$$\phi_m'' + \left(\frac{1}{\rho} - \frac{2}{3}c^2\rho\right)\phi_m' + m^2\phi_m = 0. \tag{62}$$

For $\rho \approx 0$, the term $\frac{1}{\rho}$ prevails over the term $-\frac{2}{3}c^2\rho$. Then Eq. (62) turns into a Bessel equation, whose solution is

$$\phi_{\rho\to 0}(\rho) = E_1 J_0(m\rho) + E_2 Y_0(m\rho), \tag{63}$$

where E_1 and E_2 are integration constants. Since Y_0 diverges at the origin, we set $E_2 = 0$. Thus, the behavior sketched in Fig. 6 agrees with the resulting solution.

IV. KK RESONANT MODES

Despite the fact the massive gravitational modes are not localizable on the brane, some of these modes can show a resonant profile [10,43]. The resonant states can be found by means of the resonance method [44] that consists of finding solutions of a Schrödinger equation that exhibits large amplitudes near the brane. Large peaks in the distribution of the wave function in terms of the KK masses reveal the existence of resonant states [44]. Massive particles confined on the well may be interpreted as gravitational resonant states (massive quasilocalized gravitons highly coupled to the brane) [10,38,39].

The method consists of defining the probability $P(m)$ to find a particle with mass m at the position z_0 as

$$P(m) = \frac{|\Psi_m(z_0)|^2}{\int_{z_{\min}}^{z_{\max}} |\Psi_m(z)|^2 dz}, \tag{64}$$

where $z_{\min}$ and $z_{\max}$ stand for the domain limits. An extension of this idea was proposed in Ref. [45], where a relative probability is defined as

$$P(m) = \frac{\int_{z_a}^{z_b} |\Psi_m(z)|^2 dz}{\int_{z_{\min}}^{z_{\max}} |\Psi_m(z)|^2 dz}, \tag{65}$$

evaluated in a narrow range $[z_a, z_b]$.

Probability interpretations are possible for the Sturm-Liouville eigenfunctions by defining the inner product with the weight function included. However, the change of variable $z = z(\rho)$, used to transform the Sturm-Liouville equation into a Schrödinger equation, improves the treatment for large c. By numerical integration, the change of coordinate (25) is plotted in Fig. 7. The analogue quantum potential for the GS model is

$$U_{\rm GS}(z) = 6z^{-2}. \tag{66}$$

This potential function does not support a bound state and then there is no probability of finding resonant massive gravitons in the GS model.

For the string-cigar model, the Schrödinger potential, plotted in Fig. 8, presents an infinite potential well that suggests the possibility of resonant modes. Note that for $c = 1.0$ the potential for the string-cigar model behaves as a Coulomb-like potential. As the parameter c increases, a barrier arises and the potential assumes the usual volcano shape. Furthermore, for $c \to \infty$, $U(z)$ tends to the GS model potential $U_{\rm GS}$.

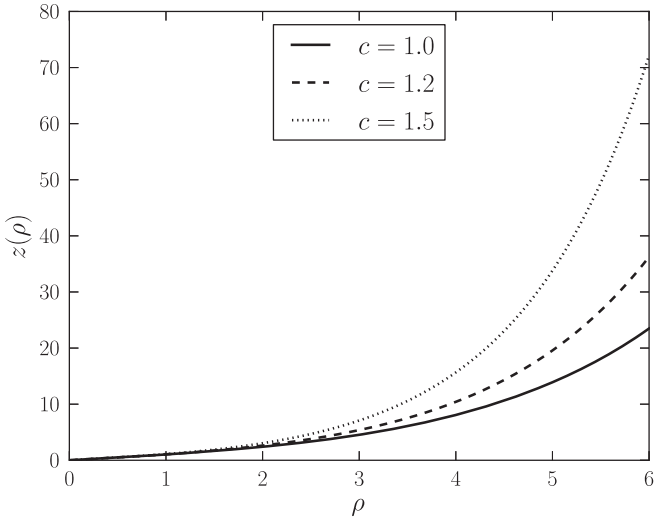

FIG. 7. Numerical integral solution of the transformation $z(\rho)$.

We solved the Schrödinger-like equation (28) using the Numerov method [46,47]. The relative probability function (65) is more suitable to detect very narrow resonances [48]. According to the energy density given at (52), the brane distribution is $[z_a, z_b] = [0.01, 0.50]$. The domain is chosen to be $[z_{\min}, z_{\max}] = [0.01, 5.0]$ (ten times the integration range), for which the plane wave probability would be $P(m) = 0.1$ [45]. The position of the resonance peak, where the physical information is stored, does not depend on $z_{\max}$, since it is chosen to be sufficiently large [48].

Figure 9 presents the numerical solution of the relative probability $P(m)$. We find, for $c = 2.9$, the first resonant

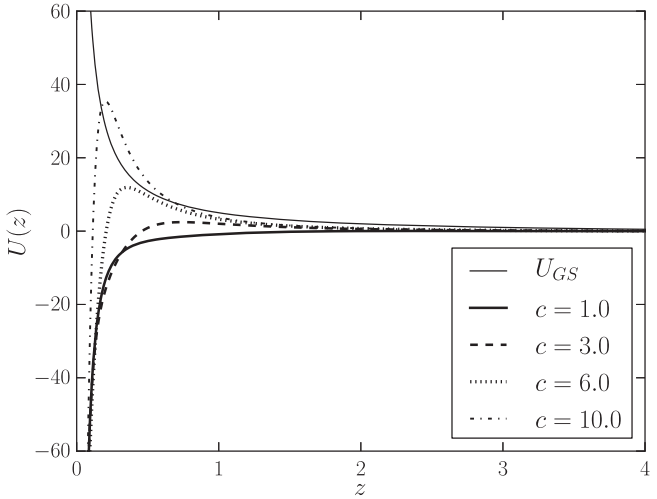

FIG. 8. The analogue quantum potential $U(z)$.

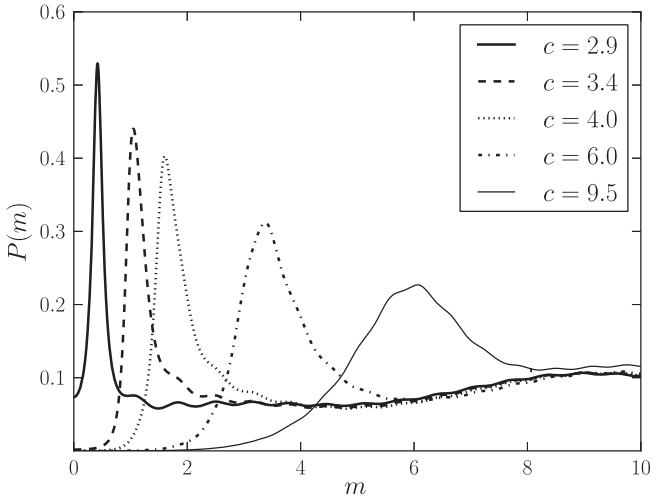

FIG. 9. Plot of the relative probability $P(m)$. The peaks reveal the resonant massive states. For $m^2 \gg U_{\max}$, a plateau is formed at $P = 0.1$ corresponding to the plane wave regime.

state. It is worthwhile to say that, as c increases, the amplitude of the resonant peaks decreases whereas the width of the probability distributions increases.

We can interpret the behavior of the resonant modes by the massive state lifetime. The lifetime of a resonant state can be estimated as $\tau \sim (\Delta m)^{-1}$, where $\Delta m = m_2 - m_1$, such that $P(m_2) = P(m_1) = \frac{1}{2}P_{\max}$ [44,49]. Therefore, for the string-cigar model, the lifetime of the resonant modes decreases when the bulk cosmological constant increases.

Figure 10 exhibits the solutions of the Schrödinger equation for the masses indicated with the probability peaks. The first solution shows that this particular massive graviton has the highest probability to be found on the brane. This solution shares a similar behavior to the zero mode presented on [27] near the origin, albeit it oscillates asymptotically with large wavelength.

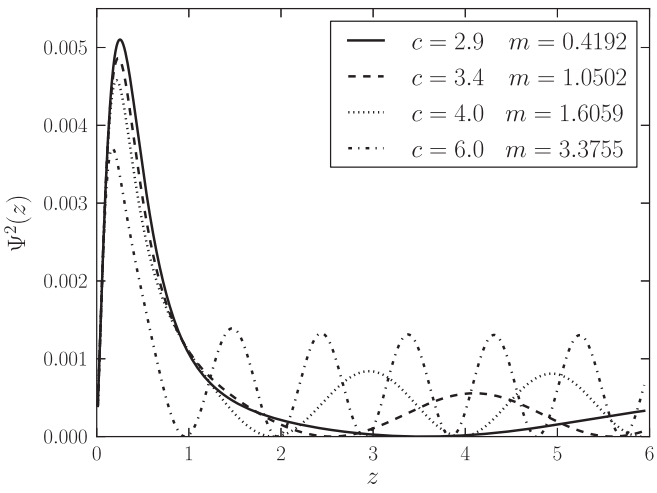

FIG. 10. Solutions of the Schrödinger-like equation for the masses corresponding to resonant peaks. The first solution has the highest probability to interact with the brane.

The effects of the brane internal structure on the resonant modes are also shown in Fig. 10. As we increase the value of c, the width of the resonance mode is enhanced. Therefore, as the brane width decreases, the resonant state lifetimes also decrease. This fact reduces the possibility of finding massive gravitons. This result agrees with the fact that for $c \to \infty$ the potential barrier tends to the $U_{\rm GS}$, where no massive state is allowed.

V. CONCLUSIONS AND PERSPECTIVES

In this work we have studied the gravitational KK modes in two stringlike braneworld scenarios, the GS and the string-cigar braneworlds. By the analysis of the energy density, the GS model can be realized as a thin-string–like model. On the other hand, the string-cigar is regarded as an interior and exterior smoothed GS model.

We have obtained a new massless mode for the GS model by analyzing the radial equation in the Schrödinger approach. It turned out that the amplitude and rate of decay of this massless mode is bigger than that of the GS model. Furthermore, we found a mass gap between the massive and massless modes for both models. It turned out that the mass gap remained constant through the Ricci flow.

We also found, via numerical analysis, the complete mass spectrum and the corresponding eigenfunctions for both models. Besides the mass gap between the massless and massive modes, both models present a gap separating two regimes in the KK spectrum. For large values of the discrete index n, the spectrum behaves linearly, as shown in Ref [19]. However, for small n, the masses decrease as $\mathbf{1/n}$. This result can be explained by the behavior of the zeros of the Bessel function of the first kind in the two regimes.

Asymptotically, the string-cigar eigenfunctions are similar to GS states. Near the brane, it turned out that the amplitude of the modes is higher in the string-cigar model than in the GS model. Hence, the brane source enhances the modes near the core.

In the GS model, the eigenfunction corresponding to the lowest mass eigenvalue resembles the massless mode with a tiny amplitude. We referred to this state as a transient mode. This mode is absent in the string-cigar braneworld. The lack of the transient mode can be regarded as a good feature of the string-cigar model since this light mode should already have been detected. Then the resolution of the GS model naturally eliminates this transient mode.

The string-cigar model allows the existence of resonant states. Indeed, the correction near the origin yields to a potential well not presented in the GS model. We found resonant modes, where the highest one occurred for $c = 2.9$ and $m = 0.4192$. As c increases the resonant lifetime decreases. The massive mode with the highest resonance peak has a high probability of interacting with the brane.

These results lead to an interesting perspective, namely, to analyze the effects of the gravitational KK modes in a correction of the Newtonian potential. In fact, the increased amplitude of the wave function at the brane core and the new decreasing behavior of the spectrum may lead to interesting modifications in the gravitational potential. Furthermore, Figs. 9–10 suggest that the first resonant peak provides a great contribution to corrections of the four-dimensional gravity laws.

Another perspective refers to the analysis of the source. The energy density profile for the string-cigar model is quite similar to the Abelian vortex model studied numerically by Giovannini *et al.* [17]. This resemblance suggests that the string-cigar geometry can be generated by a vortex with a deformed potential.

ACKNOWLEDGMENTS

The authors are grateful to the Fundação Cearense de apoio ao Desenvolvimento Científico e Tecnológico (FUNCAP), the Coordenação de Aperfeiçoamento de Pessoal de Nível Superior (CAPES), the Conselho Nacional de Desenvolvimento Científico e Tecnológico (CNPq), and the Instituto Federal do Ceará (IFCE) for financial support.

[1] L. Randall and R. Sundrum, Phys. Rev. Lett. **83**, 3370 (1999).
[2] L. Randall and R. Sundrum, Phys. Rev. Lett. **83**, 4690 (1999).
[3] N. Arkani-Hamed, S. Dimopoulos, and G. R. Dvali, Phys. Lett. B **429**, 263 (1998).
[4] I. Antoniadis, N. Arkani-Hamed, S. Dimopoulos, and G. R. Dvali, Phys. Lett. B **436**, 257 (1998).
[5] O. Klein, Z. Phys. **37**, 895 (1926); O. Klein, Ark. Mat. Astron. Fys. **34A**, 1 (1946).
[6] K. Akama, Lect. Notes Phys. **176**, 267 (1982).
[7] V. A. Rubakov and M. E. Shaposhnikov, Phys. Lett. **125B**, 136 (1983).
[8] V. A. Rubakov and M. E. Shaposhnikov, Phys. Lett. **125B**, 139 (1983).
[9] M. Visser, Phys. Lett. **159B**, 22 (1985).
[10] Martin Gremm, Phys. Lett. B **478**, 434 (2000).
[11] W. Israel, Phys. Rev. D **15**, 935 (1977); A. Vilenkin, Phys. Rev. Lett. **46**, 1169 (1981); J. Gott III, Astrophys. J. **288**, 422 (1985); W. A. Hiscock, Phys. Rev. D **31**, 3288 (1985); R. Geroch and J. Traschen, Phys. Rev. D **36**, 1017 (1987).
[12] I. Navarro and J. Santiago, J. High Energy Phys. 02 (2005) 007; I. Navarro, J. Cosmol. Astropart. Phys. 09 (2003) 004; S. Kanno and J. Soda, J. Cosmol. Astropart. Phys. 07 (2004) 002; G. Kofinas, Classical Quantum Gravity **22**, L47 (2005); G. Kofinas, Phys. Lett. B **633**, 141 (2006).
[13] R. Gregory, Phys. Rev. Lett. **59**, 740 (1987); R. Gregory, Phys. Lett. B **215**, 663 (1988); A. G. Cohen and D. B. Kaplan, Phys. Lett. B **215**, 67 (1988); G. Gibbons, M. Ortiz, and F. Ruiz, Phys. Rev. D **39**, 1546 (1989); V. P. Frolov, W. Israel, and W. G. Unruh, Phys. Rev. D **39**, 1084 (1989); R. Gregory, Phys. Rev. D **54**, 4955 (1996); M. Christensen, A. L. Larsen, and Y. Verbin, Phys. Rev. D **60**, 125012 (1999).
[14] A. G. Cohen and D. B. Kaplan, Phys. Lett. B **470**, 52 (1999).
[15] R. Gregory, Phys. Rev. Lett. **84**, 2564 (2000).
[16] I. Olasagasti and A. Vilenkin, Phys. Rev. D **62**, 044014 (2000).
[17] M. Giovannini, H. Meyer, and M. E. Shaposhnikov, Nucl. Phys. **B619**, 615 (2001).
[18] E. Ponton and E. Poppitz, J. High Energy Phys. 02 (2001) 042.
[19] T. Gherghetta and M. E. Shaposhnikov, Phys. Rev. Lett. **85**, 240 (2000).
[20] I. Oda, Phys. Lett. B **496**, 113 (2000).
[21] I. Oda, Phys. Rev. D **62**, 126009 (2000).
[22] Y. X. Liu, L. Zhao, and Y. S. L. Duan, J. High Energy Phys. 04 (2007) 097.
[23] A. Kehagias, Phys. Lett. B **600**, 133 (2004).
[24] J. Garriga and M. Porrati, J. High Energy Phys. 08 (2004) 028.
[25] M. Gogberashvili, P. Midodashvili, and D. Singleton, J. High Energy Phys. 08 (2007) 033.
[26] B. de Carlos and J. M. Moreno, J. High Energy Phys. 11 (2003) 040.
[27] J. E. G. Silva, V. Santos, and C. A. S. Almeida, Classical Quantum Gravity **30**, 025005 (2013).
[28] B. Chow, P. Lu, and L. Ni, *Hamilton's Ricci Flow* (Science Press, New York, 2006).
[29] R. S. Hamilton, The Ricci flow on surfaces, Contemporary Mathematics **71**, 237 (1988).
[30] D. Friedan, Phys. Rev. Lett. **45**, 1057 (1980); T. Oliynyk, V. Suneeta, and E. Woolgar, Nucl. Phys. **B739**, 441 (2006); A. A. Tseytlin, Phys. Rev. D **75**, 064024 (2007); T. Oliynyk, V. Suneeta, and E. Woolgar, Phys. Rev. D **76**, 045001 (2007).
[31] M. Headrick and T. Wiseman, Classical Quantum Gravity **23**, 6683 (2006).
[32] N. Lashkari and A. Maloney, Classical Quantum Gravity **28**, 105007 (2011).
[33] D. Xianzhe and L. Ma, Commun. Math. Phys. **274**, 65 (2007).
[34] P. P. Orth, P. Chandra, P. Coleman, and J. Schmalian, Phys. Rev. Lett. **109**, 237205 (2012).

[35] J. E. G. Silva and C. A. S. Almeida, Phys. Rev. D **84**, 085027 (2011).
[36] S. Randjbar-Daemi and M. E. Shaposhnikov, Phys. Lett. B **491**, 329 (2000).
[37] P. Tinyakov and K. Zuleta, Phys. Rev. D **64**, 025022 (2001).
[38] C. Csaki, J. Erlich, and T. J. Hollowood, Phys. Rev. Lett. **84**, 5932 (2000).
[39] C. Csaki, J. Erlich, T. J. Hollowood, and Y. Shirman, Nucl. Phys. **B581**, 309 (2000).
[40] A. Kehagias and K. Tamvakis, Phys. Lett. B **504**, 38 (2001).
[41] Pierluigi Amodio and Giuseppina Settanni, JNAIAM J. Numer. Anal. Indust. Appl. Math. **6**, 1 (2011).
[42] G. Watson, *A Treatise on the Theory of the Bessel Functions* (Cambridge University Press, Cambridge, 1996).
[43] A. R. Gomes, arXiv:hep-th/0611291.
[44] C. A. S. Almeida, M. M. Ferreira, Jr., A. R. Gomes, and R. Casana, Phys. Rev. D **79**, 125022 (2009).
[45] Yu-Xiao Liu, Jie Yang, Zhen-Hua Zhao, Chun-E Fu, and Yi-Shi Duan, Phys. Rev. D **80**, 065019 (2009).
[46] B. V. Numerov, Mon. Not. R. Astron. Soc. **84**, 592 (1924).
[47] B. V. Numerov, Astron. Nachr. **230**, 359 (1927).
[48] W. T. Cruz, L. S. J. Sousa, R. V. Maluf, and C. A. S. Almeida, Phys. Lett. B **730**, 314 (2014).
[49] R. Gregory, V. A. Rubakov, and S. M. Sibiryakov, Phys. Rev. Lett. **84**, 5928 (2000).